



Original Article

Identification of Natural Compounds as Potential FGFR2 Inhibitors in Cholangiocarcinoma via Virtual Screening and Network-Based Analysis

Duygu Sari-Ak¹ , Nazli Helvacı² , Fatih Con³ , Alev Kural³ ¹University of Health Sciences, Hamidiye International School of Medicine, Department of Medical Biology, Istanbul, Türkiye²University of Health Sciences, Hamidiye International School of Medicine, Department of Medical Biochemistry, Istanbul, Türkiye³University of Health Sciences, Bakirkoy Dr. Sadi Konuk Training and Research Hospital, Istanbul, Türkiye✉ **Corresponding Author:** Duygu Sari Ak (E-mail: duygusariak@gmail.com)**Received:** 2025.03.24; **Revised:** 2025.05.30; **Accepted:** 2025.06.04

Abstract

Introduction: Cholangiocarcinoma is an aggressive neoplasm of bile duct epithelial cells with poor prognosis due to limited treatment options. Fibroblast growth factor receptor 2 (FGFR2) is critical in cholangiocarcinoma by activating pathways such as MAPK/ERK and PI3K/AKT, marking it as a promising therapeutic target. This study aimed to identify natural FGFR2 inhibitors by using computational methods.

Methods: 46 natural compounds were selected from PubChem based on favorable physicochemical properties and drug-likeness criteria. Molecular docking was performed using SwissDock against FGFR2 (PDB ID: 4J97). The top five compounds were further assessed for pharmacokinetics, pharmacodynamics, and toxicity via SwissADME, pkCSM, and DeepPK tools. Additionally, protein-protein interaction networks and pathway enrichment analyses were conducted using the STRING database and KEGG.

Results: Docking analysis identified Rutecarpine, Palonosetron, Metribolone, 6-Ketoestradiol, and Gestrinone as the top FGFR2 inhibitors, with docking scores between – 6.34 and – 5.95 kcal/mol. ADMET predictions showed favorable drug-like properties, good bioavailability, and acceptable safety profiles. Network and pathway analyses confirmed FGFR2's role in key oncogenic pathways, including MAPK, PI3K/AKT, and Ras.

Conclusions: This study identified promising FGFR2 inhibitors, particularly Rutecarpine, as potential therapeutic candidates for cholangiocarcinoma, warranting further experimental validation.

Keywords: FGFR2, cholangiocarcinoma, molecular docking, natural compounds, ADMET analysis

1. Introduction

Cholangiocarcinoma (CCA), the cancer identified, is distinguished by its remarkably aggressive tendencies, originating from the bile ducts' epithelial surface, and is especially noted for its delayed identification, limited therapeutic possibilities, and unfavorable prognosis (1). In light of recent

advancements, the five-year survival percentage is still worryingly low emphasizing the necessity for groundbreaking treatment targets and improved therapeutic strategies (1,2).

The fibroblast growth factor receptor 2 (FGFR2), is a receptor tyrosine kinase and critical for

overseeing cellular development, specialization, and the mechanism of angiogenesis (3). Genetic modifications in FGFR2, comprising gene fusions and rearrangements, have been recorded in nearly 10-16% of intrahepatic CCA cases, profoundly impacting cancer formation and the disease's evolution (4). These genetic modifications render FGFR2 a crucial therapeutic target for the management of CCA (5).

Upon interaction with its ligands, FGFR2 commences a variety of signaling cascades that are fundamental to tumorigenesis and its advancement. The exploration into this subject's pathway enrichment analysis has underscored crucial signaling routes linked to FGFR2 and its partners, notably the PI3K-Akt signaling route, the MAPK signaling route, the Rap1 signaling route, and the Ras signaling route. Imbalances within these pathways are extensively recorded to promote activities such as cellular growth, endurance, new blood vessel development, and tumor spread, confirming their significance in cancer therapy (6-14).

At present, several FGFR inhibitors, including pemigatinib and infigratinib, have received approval for clinical application in the context of FGFR2-altered CCA (15,16). However, the development of resistance and adverse side effects significantly curtail their therapeutic efficacy (17,18). Consequently, the identification of novel FGFR2 inhibitors with enhanced pharmacological properties remains of paramount importance.

Within this present investigation, we executed a unified *in silico* framework that involved molecular docking (SwissDock, Lausanne, Switzerland) (19-22), evaluations regarding absorption, distribution, metabolism, excretion, and toxicity (ADMET) utilizing SwissADME (Swiss Institute of Bioinformatics, Lausanne, Switzerland) (23), pkCSM (Cambridge Centre for Computational Chemical Engineering, Cambridge, UK) (24), and DeepPK (BioSIG Lab, University of Queensland, Brisbane, Australia) (25), along with protein-protein interaction (PPI) network analysis using the STRING database (Swiss Institute of Bioinformatics, Lausanne, Switzerland) to identify natural compounds with potential inhibitory activity against FGFR2 [26]. The enrichment analysis provides valuable insights into the biological processes and signaling pathways involving FGFR2 interactions,

enhancing our understanding of their potential therapeutic impacts in CCA (27-29).

Therefore, the primary aim of this study was to identify natural compounds with high binding affinity and favorable pharmacokinetic profiles as potential FGFR2 inhibitors for the treatment of CCA. Specifically, the objectives were to conduct molecular docking simulations in order to assess the binding potential of selected natural compounds against FGFR2, to evaluate their ADMET profiles using multiple computational tools, and to explore the biological significance of FGFR2 and its interactors through protein-protein interaction and pathway enrichment analyses. These efforts collectively aim to propose viable lead compounds that enhance further experimental validation for therapeutic development.

2. Methods

2.1. Study Design

This study utilized an integrated *in silico* approach combining molecular docking, pharmacokinetic prediction (ADMET), PPI network, and enrichment analysis to identify potential natural inhibitors targeting FGFR2.

2.2. Compound Selection

Natural compounds were retrieved from the PubChem database (National Center for Biotechnology Information, Bethesda, MD, USA) by applying a multi-parameter filtering strategy to ensure drug-likeness and optimal physicochemical properties suitable for oral bioavailability: molecular weight (280-330 g/mol), H-bond acceptors (≤ 3), H-bond donors (≤ 2), rotatable bonds (≤ 3), polar surface area ($\leq 60 \text{ \AA}^2$), and XLogP (0-3). Molecular weight between 280-330 g/mol to fall within the range favorable for permeability and metabolic stability. Hydrogen bond acceptors ≤ 3 and hydrogen bond donors ≤ 2 , to comply with the topological constraints required for membrane permeability and bioavailability, in accordance with Lipinski's Rule of Five. Rotatable bonds ≤ 3 , which reduces conformational flexibility and improves binding specificity. Polar surface area (PSA) $\leq 60 \text{ \AA}^2$, as lower PSA is associated with better cell membrane permeability, especially for passive diffusion. XLogP between 0 and 3, which reflects a

balance between aqueous solubility and lipophilicity, critical for drug absorption and systemic distribution.

These criteria were selected based on widely accepted principles of medicinal chemistry and drug discovery. They are known to enhance the likelihood of identifying compounds with favorable ADME (Absorption, Distribution, Metabolism, and Excretion) profiles and were also supported by previously published studies that successfully applied similar thresholds in virtual screening campaigns (30-33).

2.3. Molecular Docking Analysis

The three-dimensional crystal structure of FGFR2 was retrieved from the Protein Data Bank (PDB ID: 4J97), representing the extracellular domain of FGFR2 in complex with FGF2. Molecular docking simulations were carried out using SwissDock (Swiss Institute of Bioinformatics, Lausanne, Switzerland), utilizing the EADock DSS engine integrated with AutoDock Vina scoring function. Docking calculations were performed across all four chains (A, B, C, and D) of the FGFR2 tetramer to capture all possible binding conformations (19-22).

The top-ranked binding poses were selected based on the fullfitness score and estimated binding free energy (ΔG , kcal/mol). For each docking result, the binding cavity and specific interaction residues were examined to determine pose validity and relevance. To validate the docking results, we utilized PoseView (ProteinsPlus, Bioinformatics Center, Hamburg, Germany) to generate 2D interaction diagrams, highlighting key residues involved in ligand binding. Furthermore, DoGSiteScorer (ProteinsPlus, Bioinformatics Center, Hamburg, Germany) was employed to assess the druggability of the identified binding pockets, analyzing their size, shape, and physicochemical properties. These tools have been validated in previous studies, demonstrating their effectiveness in predicting binding interactions and assessing pocket druggability (34-37). Interaction profiling, including hydrogen bonds, hydrophobic interactions, π -stacking, and electrostatic contacts, was performed using the PoseView tool, which provided detailed 2D schematic diagrams of protein-ligand contacts (38-41).

In particular, Rutecarpine, the top-scoring molecule, was further analyzed for binding pose validation using

DoGSiteScorer to confirm its positioning within a druggable cavity of FGFR2 and to evaluate the geometric fit of the ligand. This approach enabled precise identification of key residues (e.g., Glu565B, Leu487B, Leu633B, Ala567B, Asn571B, Arg630B) involved in the stabilization of the ligand-receptor complex, which are critical for rational drug design and understanding molecular mechanisms of inhibition (37,42).

2.4. ADMET Prediction

ADMET properties of the top five candidate molecules were analyzed by using SwissADME (Swiss Institute of Bioinformatics, Lausanne, Switzerland), pkCSM (University of Melbourne, Melbourne, Australia), and Deep-PK software (University of Queensland, Brisbane, Australia) (23-25). Predicted parameters included gastrointestinal (GI) absorption, blood-brain barrier (BBB) permeability, P-glycoprotein (P-gp) substrate and inhibition, cytochrome P450 (CYP) interactions, hepatotoxicity, and general toxicity.

2.5. Protein-Protein Interaction Network Analysis

The PPI network analysis of FGFR2 was performed using the STRING database version 11.5 (ELIXIR, Zürich, Switzerland), which integrates known and predicted protein interactions. Proteins with interaction scores above 0.7 were considered significant and included for further enrichment analysis (26).

2.6. Enrichment Analysis

KEGG (Kyoto Encyclopedia of Genes and Genomes) pathway enrichment analysis was conducted on the significant interactors obtained from STRING by using Enrichr (Icahn School of Medicine at Mount Sinai, New York, NY, USA). Pathways were considered significantly enriched with an adjusted p-value less than 0.05 (27-29).

2.7. Data Analysis

Docking scores and ADMET properties were statistically analyzed to discern significant differences among top-ranking compounds. ANOVA followed by Tukey's post-hoc test demonstrated statistically significant differences in binding affinities ($p < 0.05$), notably emphasizing Rutecarpine's superior docking performance compared to other evaluated candidates

Docking affinity scores and ADMET predictions were compared and ranked to identify the most promising FGFR2 inhibitors. Data visualization and statistical analyses were performed by using Microsoft Excel (Microsoft Corporation, Redmond, WA, USA) with in-built statistical functions and charting tools.

3. Results

3.1 Molecular Docking Analysis

The molecular docking analysis identified several natural compounds with significant binding

affinities towards the FGFR2 active site. The docking scores of the top five compounds are summarized in Table 1. The compound Rutecarpine demonstrated the strongest binding affinity (-6.348 kcal/mol), followed by Palonosetron (-6.223 kcal/mol), Metribolone (-6.032 kcal/mol), 6-Ketoestradiol (-6.029 kcal/mol), and Gestrinone (-5.959 kcal/mol). Fig 1 specifically illustrates the optimal binding mode and detailed interaction profile of Rutecarpine within the FGFR2 active site.

Table 1. Docking scores and binding affinities of the 46 natural compounds screened as potential FGFR2 inhibitors.

	Molecule Names	Best Score	Top 5 Models (Calculated Affinity (kcal/mol))
1	Rutecarpine	-6,348	-6.348, - 6.065, - 6.014, - 5.989, - 5.945
2	Palonosetron	-6,223	-6.223, - 6.153, - 5.764, - 5.403, - 5.339
3	Metribolone	-6,032	-6.032, - 5.960, - 5.631, - 5.581, - 5.436
4	6-Ketoestradiol	-6,029	-6.029, - 5.523, - 5.515, - 5.464, - 5.396
5	Gestrinone	-5,959	-5.959, - 5.266, - 5.034, - 5.002, - 4.958
6	Adrenosterone	-5,839	-5.839, - 5.590, - 5.493, - 5.297, - 5.287
7	Trenbolone Acetate	-5,826	-5.826, - 5.448, - 5.433, - 5.336, - 5.294
8	Tibolone	-5,808	-5.808, - 5.358, - 5.333, - 5.167, - 4.972
9	Androstenedione	-5,788	-5.788, - 5.688, - 5.441, - 5.167, - 5.162
10	Ondansetron	-5,764	-5.764, - 5.400, - 5.347, - 5.170, - 5.108
11	Praziquantel	-5,748	-5.748, - 5.681, - 5.678, - 5.667, - 5.632
12	Norethindrone	-5,691	-5.691, - 5.180, - 5.008, - 4.949, - 4.934
13	Gelsemine	-5,674	-5.674, - 5.415, - 5.296, - 5.254, - 5.239
14	16alpha,17-Epoxyprogesterone	-5,661	-5.661, - 5.453, - 5.255, - 5.186, - 5.107
15	Midazolam	-5,645	-5.645, - 5.430, - 5.320, - 5.203, - 5.199
16	Norquetiapine	-5,616	-5.616, - 5.578, - 5.483, - 5.314, - 5.185
17	Eburnamonine	-5,614	-5.614, - 5.430, - 5.412, - 5.362, - 5.352
18	Indoprofen	-5,592	-5.592, - 5.378, - 5.247, - 5.235, - 5.224
19	Boldione	-5,584	-5.584, - 5.581, - 5.340, - 5.253, - 5.175
20	Nile Blue Cation	-5,576	-5.576, - 5.476, - 5.411, - 5.401, - 5.276
21	4-Androsten-3β-Ol-17-One	-5,574	-5.574, - 5.405, - 5.401, - 5.285, - 5.044
22	Formestane	-5,568	-5.568, - 5.395, - 5.393, - 5.263, - 5.243
23	Lerisetron	-5,542	-5.542, - 5.486, - 5.467, - 5.436, - 5.320
24	Altrenogest	-5,535	-5.535, - 5.515, - 5.348, - 5.340, - 5.340
25	Gestodiene	-5,494	-5.494, - 5.341, - 5.018, - 4.968, - 4.961
26	Zolpidem	-5,491	-5.491, - 5.439, - 5.279, - 5.139, - 4.998
27	Cinchonine	-5,486	-5.486, - 5.306, - 5.249, - 5.132, - 5.072
28	19-Hydroxyandrost-4-Ene-3,17-Dione	-5,427	-5.427, - 5.288, - 5.099, - 4.968, - 4.892
29	Cinchonidine	-5,321	-5.321, - 5.130, - 5.116, - 5.049, - 4.961
30	4-Bromo-2,2':6',2''-Terpyridine	-5,321	-5.321, - 5.203, - 5.181, - 5.009, - 4.995
31	Granisetron	-5,307	-5.307, - 5.288, - 5.204, - 4.967, - 4.946
32	Alprazolam	-5,266	-5.266, - 5.257, - 5.147, - 5.098, - 5.071
33	2-(Chloromethyl)-3-(4-Fluorophenyl)Quinazolin-4(3H)-One	-5,24	-5.240, - 5.138, - 5.067, - 4.958, - 4.877
34	1,3-Dicyclohexylbarbituric Acid	-5,225	-5.225, - 5.037, - 4.981, - 4.969, - 4.950
35	Mazindol	-5,196	-5.196, - 5.114, - 4.988, - 4.935, - 4.877
36	1-(6-Chloro-2-Hydroxy-4-Phenylquinolin-3-Yl)Ethanone	-5,185	-5.185, - 4.994, - 4.894, - 4.855, - 4.848
37	1,4-Dibenzoylpiperazine	-5,128	-5.128, - 5.109, - 5.059, - 5.057, - 5.052
38	Methylene Blue Cation	-4,778	-4.778, - 4.705, - 4.685, - 4.616, - 4.603
39	Demoxepam	-4,513	-4.513, - 4.336, - 4.202, - 4.188, - 4.181

40	2-(3-Bromo-2-Oxopropyl)Isoindoline-1,3-Dione	-4,491	-4.491, -4.462, -4.348, -4.290, -4.247
41	Norfludiazepam	-4,439	-4.439, -4.313, -4.074, -4.001, -3.952
42	3,5-Dibromo-2-Hydroxybenzoic Acid	-4,118	-4.118, -4.093, -3.926, -3.898, -3.896
43	3,5-Dibromo-2-Methoxybenzoic Acid	-3,938	-3.938, -3.931, -3.852, -3.813, -3.766
44	5-Iodo-A-85380	-3,938	-3.938, -3.926, -3.848, -3.692, -3.636
45	1,3-Dibromo-5,5-Dimethylhydantoin	-3,567	-3.567, -3.513, -3.481, -3.434, -3.431
46	Tribromoacetic Acid	-2,994	-2.994, -2.971, -2.960, -2.853, -2.845

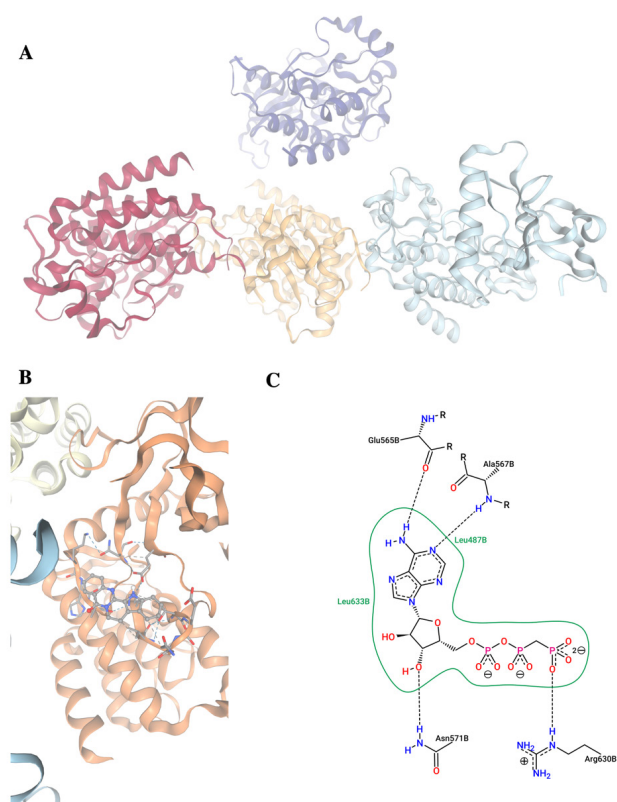


Figure 1. Molecular docking and interaction profile of Rutecarpine with FGFR2 protein (PDB ID: 4J97). A. Three-dimensional structure of the FGFR2 protein tetramer composed of four distinct chains (Chain A: red, Chain B: beige, Chain C: purple, Chain D: blue). B. Three-dimensional representation of Rutecarpine bound within the active site of FGFR2, highlighting hydrogen bonds (blue dashed lines) and hydrophobic interactions (gray dashed lines). C. Detailed two-dimensional interaction map generated by PoseView analysis, illustrating specific amino acid interactions of Rutecarpine with FGFR2. Hydrogen bonds are depicted by black dashed lines, and hydrophobic interactions are represented by green lines. Key interacting amino acid residues (Glu565, Ala567, Leu487, Leu633, Asn571, Arg630) are clearly indicated.

This comprehensive table includes the names of candidate molecules, their best docking scores

(expressed in kcal/mol), and the energies of their top five docking poses. Docking simulations were performed by using SwissDock, and the binding energies reflect the stability and strength of interactions between the ligands and the FGFR2 active site, with lower (more negative) values indicating higher affinity. The compounds were ranked from strongest to weakest binding affinity.

Rutecarpine, the top-ranked compound based on docking analysis, exhibited robust interactions within the FGFR2 active site. Detailed visualization of the molecular interactions revealed critical residues involved in binding. Specifically, Rutecarpine formed hydrogen bonds with Glu565, Ala567, Asn571, and Arg630, while establishing hydrophobic contacts with Leu487 and Leu633 (Fig 1C). These interactions underscore Rutecarpine's potential efficacy as an FGFR2 inhibitor, warranting further investigation in preclinical studies.

3.2 ADMET Profiling

Comprehensive ADMET predictions were conducted for the top five compounds using SwissADME, pkCSM, and Deep-PK tools. Results from these analysis were summarized in Table 2. Palonosetron and Rutecarpine showed notably high GI absorption and favorable BBB permeability, indicative of promising pharmacokinetic profiles. Additionally, all top candidates conformed to Lipinski's rule of five, suggesting potential for good oral bioavailability.

Table 2. Updated ADMET Profile Summary of the Top 5 Compounds (Rutecarpine, Palonosetron, Metribolone, 6-Ketoestradiol, Gestrinone).

ADMET Properties	Rutecarpine	Palonosetron	Metribolone	6-Ketoestradiol	Gestrinone
Lipinski Rule Compliance	Yes	Yes	Yes	Yes	Yes
GI Absorption	High	High	High	High	High
BBB Permeability	Yes	Yes	Yes	Yes	Yes
Caco-2 Permeability (log Papp, 10 ⁻⁶ cm/s)	1.26	1.12	1.57	1.27	1.64
Water Solubility (log mol/L)	-3.46	-2.64	-4.15	-3.60	-4.46
P-glycoprotein Substrate	Yes	Yes	No	No	No
CYP450 Enzyme Inhibition	CYP1A2, CYP2D6, CYP3A4	CYP2D6	CYP2C19	CYP2D6	CYP2C19, CYP2C9, CYP3A4
AMES Toxicity	Yes	No	No	No	No
Hepatotoxicity	Yes	Yes	No	No	No
Skin Sensitisation	No	No	No	No	No
Max. Tolerated Dose (human, log mg/kg/day)	0.068	-0.453	-0.135	-0.544	-0.395
Synthetic Accessibility	2.78	4.37	4.92	3.60	5.26

The table summarizes the pharmacokinetic (ADMET) profiles of the top five selected compounds: Rutecarpine, Palonosetron, Metribolone, 6-Ketoestradiol, and Gestrinone. ADMET parameters, including Lipinski Rule compliance, GI absorption, BBB permeability, Caco-2 permeability, water solubility, interactions with drug transporters (P-glycoprotein), metabolic enzyme inhibition (CYP450 enzymes), and toxicity profiles (AMES toxicity, hepatotoxicity, skin sensitization, maximum tolerated dose), were evaluated by using integrated computational tools (SwissADME, pkCSM, and Deep-PK). These data provide valuable insights into their potential suitability as drug candidates, focusing on efficacy, pharmacological profile, safety, and synthetic accessibility.

3.3 Protein-Protein Interaction and Enrichment Analysis

Protein-protein interaction network analysis via STRING revealed nine proteins significantly interacting with FGFR2, namely FGF1, FGF2, FGF7, FGF8, FGF9, FGF10, FGFR3, GRB2, and PLCG1 (Fig 2). Pathway enrichment analysis utilizing KEGG pathways further highlighted critical involvement in MAPK signaling, PI3K-Akt signaling, and Ras signaling pathways, which were summarized in Table 3.

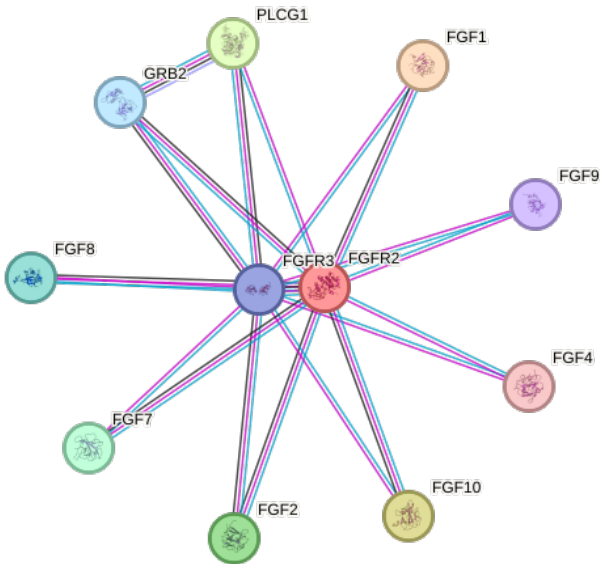


Figure 2. Protein-Protein Interaction Network Analysis of FGFR2. The interaction network demonstrates significant protein interactions involving FGFR2. Notably, strong connections were observed between FGFR2 and various fibroblast growth factors (FGFs), including FGF1, FGF2, FGF7, FGF8, FGF9, and FGF10. Additionally, FGFR2 interactions with FGFR3, another receptor involved in related signaling pathways, and essential adaptor or signaling proteins such as GRB2 and PLCG1, were illustrated. The analysis was conducted using the STRING database, in which nodes represent proteins, edges represented protein-protein interactions, and thicker lines indicate stronger associations. These interactions highlight critical signaling pathways potentially impacted by FGFR2 inhibition.

Table 3. KEGG Pathway Enrichment Analysis of FGFR2-Interacting Proteins.

Pathway	Overlap	P-value	Adjusted P-value	Genes
Ras signaling	9/232	3.25E-18	2.60E-16	FGF7, FGF8, FGF9, GRB2, PLCG1, FGF1, FGF2, FGFR3, FGF10
Rap1 signaling pa	8/210	1.15E-15	4.61E-14	FGF7, FGF8, FGF9, PLCG1, FGF1, FGF2, FGFR3, FGF10
Calcium signaling	8/240	3.41E-15	9.09E-14	FGF7, FGF8, FGF9, PLCG1, FGF1, FGF2, FGFR3, FGF10
Pathways in cancer	9/531	6.13E-15	1.23E-13	FGF7, FGF8, FGF9, GRB2, PLCG1, FGF1, FGF2, FGFR3, FGF10
MAPK signaling	8/294	1.76E-14	2.82E-13	FGF7, FGF8, FGF9, GRB2, FGF1, FGF2, FGFR3, FGF10
Breast cancer	7/147	3.57E-14	4.49E-13	FGF7, FGF8, FGF9, GRB2, FGF1, FGF2, FGF10
Gastric cancer	7/149	3.93E-14	4.49E-13	FGF7, FGF8, FGF9, GRB2, FGF1, FGF2, FGF10
PI3K-Akt signaling	8/354	7.89E-14	7.89E-13	FGF7, FGF8, FGF9, GRB2, FGF1, FGF2, FGFR3, FGF10
Melanoma	6/72	1.46E-13	1.30E-12	FGF7, FGF8, FGF9, FGF1, FGF2, FGF10
Regulation of actin cytoskeleton	7/218	5.86E-13	4.69E-12	FGF7, FGF8, FGF9, FGF1, FGF2, FGFR3, FGF10

The table summarizes the significantly enriched KEGG pathways associated with proteins interacting with FGFR2, including FGF1, FGF2, FGF7, FGF8, FGF9, FGF10, FGFR3, GRB2, and PLCG1. Pathways were ranked according to statistical significance (p-value). The analysis highlights critical signaling pathways such as MAPK, Ras, PI3K-Akt, and Rap1, which are involved in cancer progression and cellular proliferation. The enrichment analysis was performed using Enrichr software.

Docking scores and ADMET properties were statistically analyzed to discern significant differences among top-ranking compounds. ANOVA followed by Tukey's post-hoc test demonstrated statistically significant differences in binding affinities ($p < 0.05$), notably emphasizing Rutecarpine's superior docking performance compared to other evaluated candidates (Fig 3).

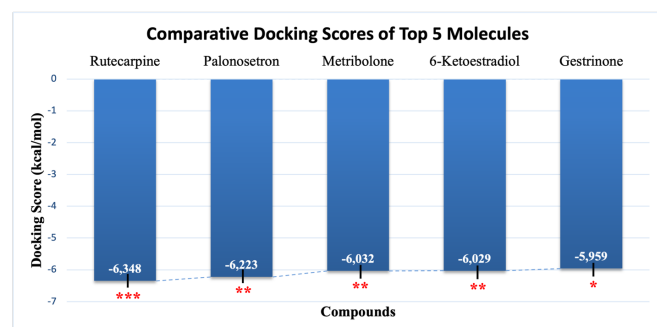


Figure 3. Comparative Docking Scores of Top Five Molecules Against FGFR2. Docking scores for Rutecarpine, Palonosetron, Metribolone, 6-Ketoestradiol, and Gestrinone are displayed with respective standard deviations. Statistical significance (ANOVA, Tukey's post-hoc test) is indicated by red asterisks (* $p < 0.05$, ** $p < 0.01$, *** $p < 0.001$). Rutecarpine exhibited significantly stronger binding affinity compared to other evaluated molecules, highlighting its superior potential as an FGFR2 inhibitor candidate.

4. Discussion

This study provides a comprehensive *in silico* evaluation of natural compounds as potential FGFR2 inhibitors for CCA, an aggressive cancer with limited therapeutic options and poor prognosis (1,2). FGFR2 has emerged as a critical oncogenic driver, with gene fusions and amplifications contributing to CCA pathogenesis in approximately 10-16% of cases (3-5).

Our molecular docking analysis identified Rutecarpine as the lead compound, exhibiting the highest binding affinity (-6.348 kcal/mol). Detailed analysis of Rutecarpine's binding mode revealed stable interactions within the FGFR2 active site, including hydrogen bonds with key residues such as Glu565, Ala567, Asn571, and Arg630, and hydrophobic contacts involving Leu487 and Leu633. These interactions, distributed across multiple chains of the FGFR2 tetramer, suggest a robust inhibition mechanism that could effectively disrupt FGFR2-mediated oncogenic signaling, potentially enhancing therapeutic outcomes.

The application of validated computational tools such as PoseView and DoGSiteScorer enhances the credibility of our *in silico* findings. PoseView's detailed interaction mappings provide insights into the specific residues involved in ligand binding, while DoGSiteScorer's assessment of pocket druggability offers a quantitative evaluation of the binding site's suitability for therapeutic targeting. The reliability of these tools has been established in prior research, supporting their integration into our study's methodology.

By incorporating these validated methods, we have strengthened the robustness of our computational analysis, providing a solid foundation for the proposed therapeutic potential of the identified compounds.

ADMET predictions further support the drug-likeness of Rutecarpine. Its high gastrointestinal absorption and favorable pharmacokinetic properties make it a strong candidate for oral administration. However, hepatotoxicity and AMES toxicity risks warrant caution and suggest the need for structural modifications or further preclinical studies to ensure safety.

When compared to previous research, our findings align with the well-established principle that natural products are valuable scaffolds for drug discovery, particularly in oncology. Palonosetron, a clinically approved antiemetic, also showed favorable ADMET profiles and significant binding to FGFR2, suggesting a potential repositioning opportunity for targeting CCA.

The protein-protein interaction network analysis revealed FGFR2's association with key oncogenic signaling mediators such as FGFR3, GRB2, and PLCG1, as well as with multiple fibroblast growth factors. KEGG pathway enrichment analysis highlighted critical pathways (MAPK, PI3K-Akt, Ras, and Rap1), all of which are commonly dysregulated in CCA and other solid tumors (6-14). The dual targeting of FGFR2 and its interactors could enhance therapeutic efficacy by disrupting tumor-promoting pathways and reducing the potential for resistance.

While FGFR inhibitors like pemigatinib and infigratinib have advanced clinical outcomes, their use is often hampered by resistance development and adverse events (15-18). Rutecarpine's multi-site binding profile within the FGFR2 tetramer may overcome some of these limitations by stabilizing FGFR2 in an inactive conformation or preventing dimerization-dependent activation.

Strengths of this study include the integration of molecular docking, ADMET profiling, PPI network analysis, and pathway enrichment, which collectively provide a holistic understanding of Rutecarpine's potential. However, limitations must also be acknowledged: (i) *in silico* predictions require

validation through *in vitro* and *in vivo* studies, (ii) predicted hepatotoxicity raises concerns about safety, and (iii) dynamic factors such as metabolic biotransformation were not directly modeled.

Future studies should focus on experimental validation of Rutecarpine's inhibitory effect on FGFR2 phosphorylation, downstream signaling suppression, and cytotoxicity in CCA cell lines. *In vivo* pharmacokinetic studies will also be critical to confirm absorption, distribution, metabolism, and excretion properties.

This study identifies Rutecarpine as a promising FGFR2 inhibitor with significant potential for further drug development targeting CCA. The results of this study contribute to the growing body of evidence supporting natural compounds as valuable sources for anticancer therapeutics and underscore the importance of targeting FGFR2-mediated signaling in CCA.

5. Conclusion

In this study, we successfully identified and characterized natural compounds with promising inhibitory potential against FGFR2, a significant molecular target implicated in CCA progression. Rutecarpine emerged as the most potential candidate, exhibiting the highest binding affinity and favorable pharmacokinetic and toxicity profiles. Additional compounds, including Palonosetron, Metribolone, 6-Ketoestradiol, and Gestrinone, also demonstrated considerable inhibitory potential. Protein-protein interaction network analysis and KEGG pathway enrichment indicated that these compounds could broadly modulate oncogenic signaling pathways, such as MAPK, PI3K-Akt, and Ras signaling, reinforcing their therapeutic relevance. These findings provide robust evidence supporting the advancement of Rutecarpine and other identified compounds into further preclinical and clinical studies, potentially contributing to more effective and safer therapeutic strategies for CCA.

Conflicts of interest: The authors declare no conflicts of interest related to this work.

Ethics approval: Not applicable.

Funding: This research received no external funding.

References

- Ilyas SI, Gores GJ. Pathogenesis, Diagnosis, and Management of Cholangiocarcinoma. *Gastroenterology* 2013;145:1215-1229. <https://doi.org/10.1053/j.gastro.2013.10.013>
- Banales JM, Cardinale V, Carpino G, Marzioni M, Andersen JB, Invernizzi P, Lind GE, Folseraas T, Forbes SJ, Fouassier L, Geier A, Calvisi DF, Mertens JC, Trauner M, Benedetti A, Maroni L, Vaquero J, Macias RI, Raggi C, Perugorria MJ, Gaudio E, Boberg KM, Marin JJ, Alvaro D. Expert consensus document: Cholangiocarcinoma: current knowledge and future perspectives consensus statement from the European Network for the Study of Cholangiocarcinoma (ENS-CCA). *Nat Rev Gastroenterol Hepatol*. 2016;13:261-280. <https://doi.org/10.1038/nrgastro.2016.51>
- Turner N, Grose R. Fibroblast growth factor signalling: from development to cancer. *Nat Rev Cancer* 2010;10:116-129. <https://doi.org/10.1038/nrc2780>
- Arai Y, Totoki Y, Hosoda F, Shiota T, Hama N, Nakamura H, Ojima H, Furuta K, Shimada K, Okusaka T, Kosuge T, Shibata T. Fibroblast growth factor receptor 2 tyrosine kinase fusions define a unique molecular subtype of cholangiocarcinoma. *Hepatology* 2014;59:1427-1434. <https://doi.org/10.1038/nrc2780>
- Javle M, Lowery M, Shroff RT, Weiss KH, Springfield C, Borad MJ, Ramanathan RK, Goyal L, Sadeghi S, Macarulla T, El-Khoueiry A, Kelley RK, Borbath I, Choo SP, Oh DY, Philip PA, Chen LT, Reungwetwattana T, Van Cutsem E, Yeh KH, Ciombor K, Finn RS, Patel A, Sen S, Porter D, Isaacs R, Zhu AX, Abou-Alfa GK, Bekaii-Saab T. Phase II Study of BGJ398 in Patients With FGFR-Altered Advanced Cholangiocarcinoma. *J Clin Oncol*. 2018;36:276-282. <https://doi.org/10.1200/JCO.2017.75.5009>
- Glaviano A, Foo ASC, Lam HY, Yap KCH, Jacot W, Jones RH, Eng H, Nair MG, Makvandi P, Geoerger B, Kulke MH, Baird RD, Prabhu JS, Carbone D, Pecoraro C, Teh DBL, Sethi G, Cavalieri V, Lin KH, Javidi-Sharifi NR, Toska E, Davids MS, Brown JR, Diana P, Stebbing J, Fruman DA, Kumar AP. PI3K/AKT/mTOR signaling transduction pathway and targeted therapies in cancer. *Mol Cancer* 2023;22:138. <https://doi.org/10.1186/s12943.023.01827-6>
- Hoon DS, Furuhashi S, Mizuno S, Ryu S, Naeini YB, Bilchik AJ, Bustos MA. Spatial molecular profiling identifies FGF20 upregulation on cancer-associated fibroblast and FGFR2-PI3K/Akt activation in tumor cells of sporadic early-onset colon cancer. *Ann. Oncol*. 2023;34:S1517. <https://doi.org/10.1016/j.annonc.2023.10.258>
- Du S, Zhang Y, Xu J. Current progress in cancer treatment by targeting FGFR signaling. *Cancer Biol Med* 2023;20:490-9. <https://doi.org/10.20892/j.issn.2095-3941.2023.0137>
- Dixit G, Gonzalez-Bosquet J, Skurski J, Devor EJ, Dickerson EB, Nothnick WB, Issuree PD, Leslie KK, Maretzky T. FGFR2 mutations promote endometrial cancer progression through dual engagement of EGFR and Notch signalling pathways. *Clin Transl Med*. 2023;13. <https://doi.org/10.1002/ctm2.1223>
- Gorska-Arcisz M, Popeda M, Braun M, Piasecka D, Nowak JJ, Kitowska K, Stasiłoj G, Okroj M, Romanska HM, Sadej R. FGFR2-triggered autophagy and activation of Nrf-2 reduce breast cancer cell response to anti-ER drugs. *Cell Mol Biol Lett* 2024;29:71. <https://doi.org/10.1186/s11658.024.00586-6>
- Tam B, Severson P, Quah CS, Harding JJ. Phase I study evaluating KIN-3248, a next-generation, irreversible pan-FGFR inhibitor, in patients with advanced cholangiocarcinoma, urothelial carcinoma and other solid tumors harboring FGFR2 and/or FGFR3 gene alterations. *Ann. Oncol*. 2023;34:S231-232. <https://doi.org/10.1016/j.annonc.2023.09.1423>
- Lin X, Ding X, Bavadekar S, Rao S, Zhang M, Ren F, Zhavoronkov A. Discovery and preclinical characterization of ISM8001, a covalent and selective FGFR2/FGFR3 dual inhibitor with strong monotherapy anti-tumor activity against advanced solid tumors. *Cancer Res* 2024;84:5582-5582. <https://doi.org/10.1158/1538-7445.AM2024-5582>
- Subbiah V, Sahai V, Maglic D, Bruderek K, Touré BB, Zhao S, Valverde R, O'Hearn PJ, Moustakas DT, Schönherr H, Gerami-Moayed N, Taylor AM, Hudson BM, Houde DJ, Pal D, Foster L, Gunaydin H, Ayaz P, Sharon DA, Goyal L, Schram AM, Kamath S, Sherwin CA, Schmidt-Kittler O, Jen KY, Ricard F, Wolf BB, Shaw DE, Bergstrom DA, Watters J, Casaleto JB. RLY-4008, the First Highly Selective FGFR2 Inhibitor with Activity across FGFR2 Alterations and Resistance Mutations. *Cancer Discov* 2023;13:2012-2031. <https://doi.org/10.1158/2159-8290.CD-23-0475>
- Ornitz DM, Itoh N. The Fibroblast Growth Factor signaling pathway. *WIREs Developmental Biology* 2015;4:215-266. <https://doi.org/10.1002/wdev.176>
- Abou-Alfa GK, Sahai V, Hollebecque A, Vaccaro G, Melisi D, Al-Rajabi R, Paulson AS, Borad MJ, Gallinson D, Murphy AG, Oh DY, Dotan E, Catenacci DV, Van Cutsem E, Ji T, Lihou CF, Zhen H, Félez L, Vogel A. Pemigatinib for previously treated, locally advanced or metastatic cholangiocarcinoma: a multicentre, open-label, phase 2 study. *Lancet Oncol* 2020;21:671-684. [https://doi.org/10.1016/S1470-2045\(20\)30109-1](https://doi.org/10.1016/S1470-2045(20)30109-1)
- Meza K, Villegas De Leon S, Pant S, Tang T-Y, Meric-Bernstam F, Hu ZI, Milind MJ, Lee SS. Tumor vascularity as a predictor of FGFR inhibitor response in FGFR2-fused intrahepatic cholangiocarcinoma. *JCO* 2025;43:638-638. https://doi.org/10.1200/JCO.2025.43.4_suppl.63
- Gong J, Mita AC, Wei Z, Cheng HH, Mitchell EP, Wright JJ, Ivy SP, Wang V, Gray RC, McShane LM, Rubinstein LV, Patton DR, Williams PM, Hamilton SR, Alva AS, Tricoli JV, Conley BA, Arteaga CL, Harris LN, O'Dwyer PJ, Chen AP, Flaherty KT. Phase II Study of Erdafitinib in Patients With Tumors With FGFR Amplifications: Results From the NCI-MATCH ECOG-ACRIN Trial (EAY131) Subprotocol K1. *JCO Precis Oncol* 2024. <https://doi.org/10.1200/PO.23.00406>
- Brandi G, Relli V, Deserti M, Palloni A, Indio V, Astolfi A, Serravalle S, Mattiaccio A, Vasuri F, Malvi D, Deiana C, Abbondanza Pantaleo M, Cescon M, Rizzo A, Katoh M, Tavolari S. Activated FGFR2 signalling as a biomarker for selection of intrahepatic cholangiocarcinoma patients candidate to FGFR targeted therapies. *Sci Rep* 2024;14:3136. <https://doi.org/10.1038/s41598.024.52991-8>
- Trott O, Olson AJ. AutoDock Vina: Improving the speed and accuracy of docking with a new scoring function, efficient optimization, and multithreading. *J Comput Chem* 2010;31:455-461. <https://doi.org/10.1002/jcc.21334>
- Grosdidier A, Zoete V, Michielin O. SwissDock, a protein-small molecule docking web service based on EADock DSS. *Nucleic Acids Res* 2011;39:W270-277. <https://doi.org/10.1093/nar/gkr366>
- Eberhardt J, Santos-Martins D, Tillack AF, Forli S. AutoDock Vina 1.2.0: New Docking Methods, Expanded Force Field, and Python Bindings. *J Chem Inf Model* 2021;61:3891-3898. <https://doi.org/10.1021/acs.jcim.1c00203>
- Bugnon M, Röhrig UF, Goullieux M, Perez MAS, Daina A, Michielin O, Zoete V. SwissDock 2024: major enhancements for small-molecule docking with Attracting Cavities and

- AutoDock Vina. *Nucleic Acids Res* 2024;52:W324-332. <https://doi.org/10.1093/nar/gkae300>.
23. Daina A, Michielin O, Zoete V. SwissADME: a free web tool to evaluate pharmacokinetics, drug-likeness and medicinal chemistry friendliness of small molecules. *Sci Rep* 2017;7:42717. <https://doi.org/10.1038/srep42717>.
 24. Pires DEV, Blundell TL, Ascher DB. pkCSM: Predicting small-molecule pharmacokinetic and toxicity properties using graph-based signatures. *J Med Chem* 2015;58:4066-4072. <https://doi.org/10.1021/acs.jmedchem.5b00104>.
 25. Myung Y, de Sá AGC, Ascher DB. Deep-PK: deep learning for small molecule pharmacokinetic and toxicity prediction. *Nucleic Acids Res* 2024;52:W469-475. <https://doi.org/10.1093/nar/gkae254>.
 26. Szklarczyk D, Kirsch R, Koutrouli M, Nastou K, Mehryary F, Hachilif R, Gable AL, Fang T, Doncheva NT, Pyysalo S, Bork P, Jensen LJ, von Mering C. The STRING database in 2023: protein-protein association networks and functional enrichment analyses for any sequenced genome of interest. *Nucleic Acids Res* 2023;51:D638-D646. <https://doi.org/10.1093/nar/gkac1000>.
 27. Kuleshov MV, Jones MR, Rouillard AD, Fernandez NF, Duan Q, Wang Z, Koplev S, Jenkins SL, Jagodnik KM, Lachmann A, McDermott MG, Monteiro CD, Gundersen GW, Ma'ayan A. Enrichr: a comprehensive gene set enrichment analysis web server 2016 update. Enrichr: a comprehensive gene set enrichment analysis web server 2016 update. *Nucleic Acids Res* 2016;44:W90-97. <https://doi.org/10.1093/nar/gkw377>.
 28. Daina A, Michielin O, Zoete V. iLOGP: A Simple, Robust, and Efficient Description of n – Octanol/Water Partition Coefficient for Drug Design Using the GB/SA Approach. *J Chem Inf Model* 2014;54:3284-3301. <https://doi.org/10.1021/ci500467k>.
 29. Xie Z, Bailey A, Kuleshov MV, Clarke DJB, Evangelista JE, Jenkins SL, Lachmann A, Wojciechowicz ML, Kropiwnicki E, Jagodnik KM, Jeon M, Ma'ayan A. Gene Set Knowledge Discovery with Enrichr. *Curr Protoc* 2021;1. <https://doi.org/10.1002/cpz1.90>.
 30. Kim S, Chen J, Cheng T, Gindulyte A, He J, He S, Li Q, Shoemaker BA, Thiessen PA, Yu B, Zaslavsky L, Zhang J, Bolton EE. PubChem 2025 update. *Nucleic Acids Res* 2025;53:D1516-25. <https://doi.org/10.1093/nar/gkae1059>.
 31. Lipinski CA, Lombardo F, Dominy BW, Feeney PJ. Experimental and computational approaches to estimate solubility and permeability in drug discovery and development settings 1PII of original article: S0169-409X(96)00423-1. The article was originally published in *Advanced Drug Delivery Reviews* 23 (1997). *Adv Drug Deliv Rev* 2001;46:3-26. [https://doi.org/10.1016/S0169-409X\(00\)00129-0](https://doi.org/10.1016/S0169-409X(00)00129-0).
 32. Veber DF, Johnson SR, Cheng H-Y, Smith BR, Ward KW, Kopple KD. Molecular Properties That Influence the Oral Bioavailability of Drug Candidates. *J Med Chem* 2002;45:2615-2623. <https://doi.org/10.1021/jm020017n>.
 33. Ghose AK, Viswanadhan VN, Wendoloski JJ. A Knowledge-Based Approach in Designing Combinatorial or Medicinal Chemistry Libraries for Drug Discovery. 1. A Qualitative and Quantitative Characterization of Known Drug Databases. *J Comb Chem* 1999;1:55-68. <https://doi.org/10.1021/cc9800071>.
 34. Stierand K, Rarey M. PoseView – molecular interaction patterns at a glance. *J Cheminform* 2010;2:P50. <https://doi.org/10.1186/1758-2946-2-S1-P50>.
 35. Fährrolfes R, Bietz S, Flachsenberg F, Meyder A, Nittinger E, Otto T, Volkamer A, Rarey M. ProteinsPlus: a web portal for structure analysis of macromolecules. *Nucleic Acids Res* 2017;45:W337-343. <https://doi.org/10.1093/nar/gkx333>.
 36. Volkamer A, Kuhn D, Rippmann F, Rarey M. DoGSiteScorer: a web server for automatic binding site prediction, analysis and druggability assessment. *Bioinformatics* 2012;28:2074-2075. <https://doi.org/10.1093/bioinformatics/bts310>.
 37. Volkamer A, Kuhn D, Grombacher T, Rippmann F, Rarey M. Combining Global and Local Measures for Structure-Based Druggability Predictions. *J Chem Inf Model* 2012;52:360-372. <https://doi.org/10.1021/ci200454v>.
 38. Stierand K, Maaß PC, Rarey M. Molecular complexes at a glance: automated generation of two-dimensional complex diagrams. *Bioinformatics* 2006;22:1710-1716. <https://doi.org/10.1093/bioinformatics/btl150>.
 39. Stierand K, Rarey M. Drawing the PDB: Protein–Ligand Complexes in Two Dimensions. *ACS Med Chem Lett* 2010;1:540-545. <https://doi.org/10.1021/ml100164p>.
 40. Fricker PC, Gastreich M, Rarey M. Automated Drawing of Structural Molecular Formulas under Constraints. *J Chem Inf Comput Sci* 2004;44:1065-1078. <https://doi.org/10.1021/ci049958u>.
 41. Stierand K, Rarey M. From Modeling to Medicinal Chemistry: Automatic Generation of Two-Dimensional Complex Diagrams. *ChemMedChem* 2007;2:853-860. <https://doi.org/10.1002/cmdc.200700010>.
 42. Volkamer A, Griewel A, Grombacher T, Rarey M. Analyzing the Topology of Active Sites: On the Prediction of Pockets and Subpockets. *J Chem Inf Model* 2010;50:2041-2052. <https://doi.org/10.1021/ci100241y>.

Cite this article: Sari-Ak D, Helvacı N, Con F, Kural A. Identification of Natural Compounds as Potential FGFR2 Inhibitors in Cholangiocarcinoma via Virtual Screening and Network-Based Analysis. *Pharmedicine J.* 2025;2(2); 59-68. DOI: 10.62482/pmj.28